NANO LETTERS

LETTER

pubs.acs.org/NanoLett

Selective Sulfuration at the Corner Sites of a Silver Nanocrystal and Its Use in Stabilization of the Shape

Jie Zeng,[†] Jing Tao,[‡] Dong Su,[§] Yimei Zhu,[‡] Dong Qin,[∥] and Younan Xia*[,†]

[†]Department of Biomedical Engineering, Washington University, St. Louis, Missouri 63130, United States

[‡]Condensed Matter Physics and Materials Science Department and [§]Center for Functional Nanomaterials, Brookhaven National Laboratory, Upton, New York 11973, United States

[∥]Nano Research Facility, Department of Energy, Environmental, and Chemical Engineering, Washington University, St. Louis, Missouri 63130, United States

Supporting Information

ABSTRACT: This paper describes a new approach to site-selective sulfuration at the corner sites of Ag nanocrystals including triangular nanoplates and nanocubes. The reaction simply involved mixing an aqueous suspension of the Ag nanocrystals with an aqueous solution of polysulfide at room temperature. As a precursor to elemental S, polysulfide is highly soluble in water and can directly react with elemental Ag upon contact to generate Ag_2S in the absence of oxygen. The reaction was easily initiated at the corner sites and then pushed toward the center. By controlling the reaction time and/or the amount of polysulfide added, the reaction could be confined to the corner sites only, generating Ag−Ag_2S hybrid nanocrystals with greatly improved stability against aging at 80 and 100 °C in air than their counterparts made of pure Ag.

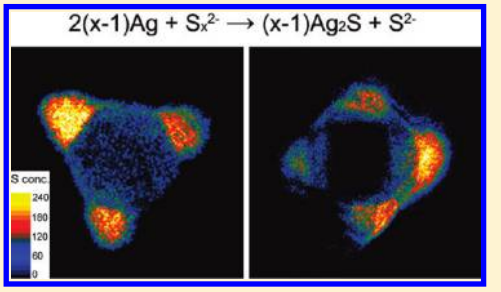

KEYWORDS: Site-selection, sulfuration, polysulfide, silver, nanocrystals, stability

Silver nanocrystals with well-defined and controllable shapes have received great interests in recent years due to their intriguing properties and potential applications in a number of areas including catalysis, photonics, electronics, and optical sensing/labeling/imaging.[1−8] Thanks to the efforts from many research groups, Ag nanocrystals with a rich variety of different shapes have been synthesized with notable examples including cubes, plates, wires, rods, bars, right bipyramids, octahedrons, decahedrons, and asymmetrically truncated octahedrons.[9−19] Most of these nanocrystals contain sharp features on the surface and are therefore unstable from the viewpoint of thermodynamics. They are expected to spontaneously evolve into new forms (e.g., spheres and circular disks) with lower surface energies over different time scales.[8,20−22] As an immediate consequence of this shape transformation, the nanocrystal may lose its originally designed electronic, optical, and catalytic properties. For example, Ag nanoplates display a strong, in-plane dipole resonance mode in the near-infrared region, but its peak position is highly sensitive to the sharpness of the corners.[8,22] As the corners become rounded, the peak position will experience significant blue shifts by as much as 300 nm.[8,22] In a different case, Ag nanocubes enclosed by {100} facets have been demonstrated as a superb catalyst for epoxidation,[4,23] but the selectivity of this catalytic reaction tends to drop drastically as the cubes become rounded at the corners to expose {111} facets.[23] It is still a grand challenge to preserve the shape of a nanocrystal with sharp features on the surface.

Herein, we report a new strategy for preserving the shape of a Ag nanoplate or nanocube via selective sulfuration of the sharp corners. Previously, Song and co-workers reported the synthesis of Ag_2S−Au−Ag_2S nanorods through a reaction between Ag−Au−Ag nanorods and Na_2S (or S^{2-}) in the presence of oxygen.[24] The reaction progressed so rapidly that the entire Ag segments of each nanorod were completely transformed into Ag_2S within 1 min. Most recently, a similar approach was used by Ma and co-workers to achieve partial sulfuration of triangular Ag nanoplates with truncated corners.[25] However, it was still difficult to control the kinetics of sulfuration, and the morphology of the final product was found to deviate from the original shape possibly due to the involvement of oxidation of Ag to Ag^+, which then reacted with S^{2-} to generate Ag_2S. Here we demonstrate an effective strategy for maneuvering the sulfuration kinetics by using a polysulfide (Na_2S_x) to react with Ag nanocrystals at room temperature. As a precursor to elemental S, Na_2S_x is highly soluble in water and can directly react with elemental Ag upon contact to generate Ag_2S even in the absence of oxygen. Significantly, we could easily and tightly control the kinetics and degree of sulfuration to obtain Ag−Ag_2S hybrid nanocrystals with Ag_2S only being formed at the corner sites.

Received: May 16, 2011
Revised: June 13, 2011
Published: June 20, 2011

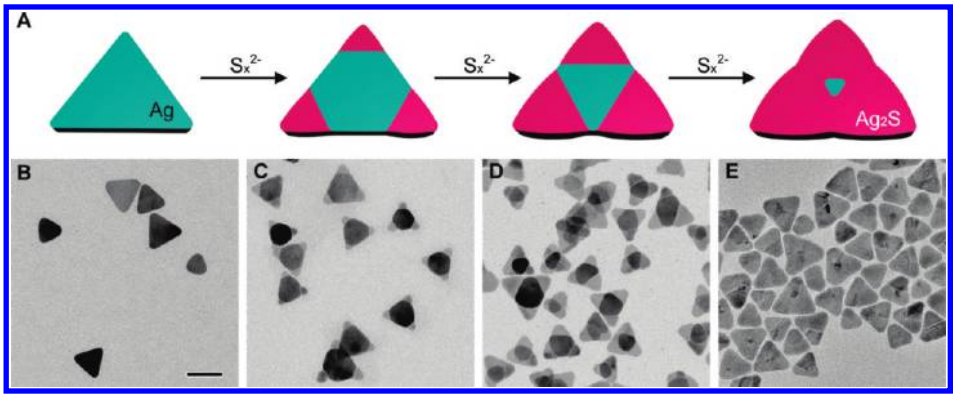

Figure 1. Progression of the site-selected reaction between a triangular Ag nanoplate and S_x^{2-} ions. (A) Schematic illustration of the sulfuration reaction, by which elemental Ag reacts with S_x^{2-} in water to generate Ag_2S under the ambient conditions of a laboratory. (B) TEM image of the triangular Ag nanoplates with slight truncation at all corners. (C–E) TEM images of the products obtained after the sulfuration reaction had progressed for (C) 1, (D) 5, and (E) 20 min. The dark region in the center corresponds to Ag while the gray regions at corner sites correspond to Ag_2S. The scale bar is 50 nm in (B) and applies to all images.

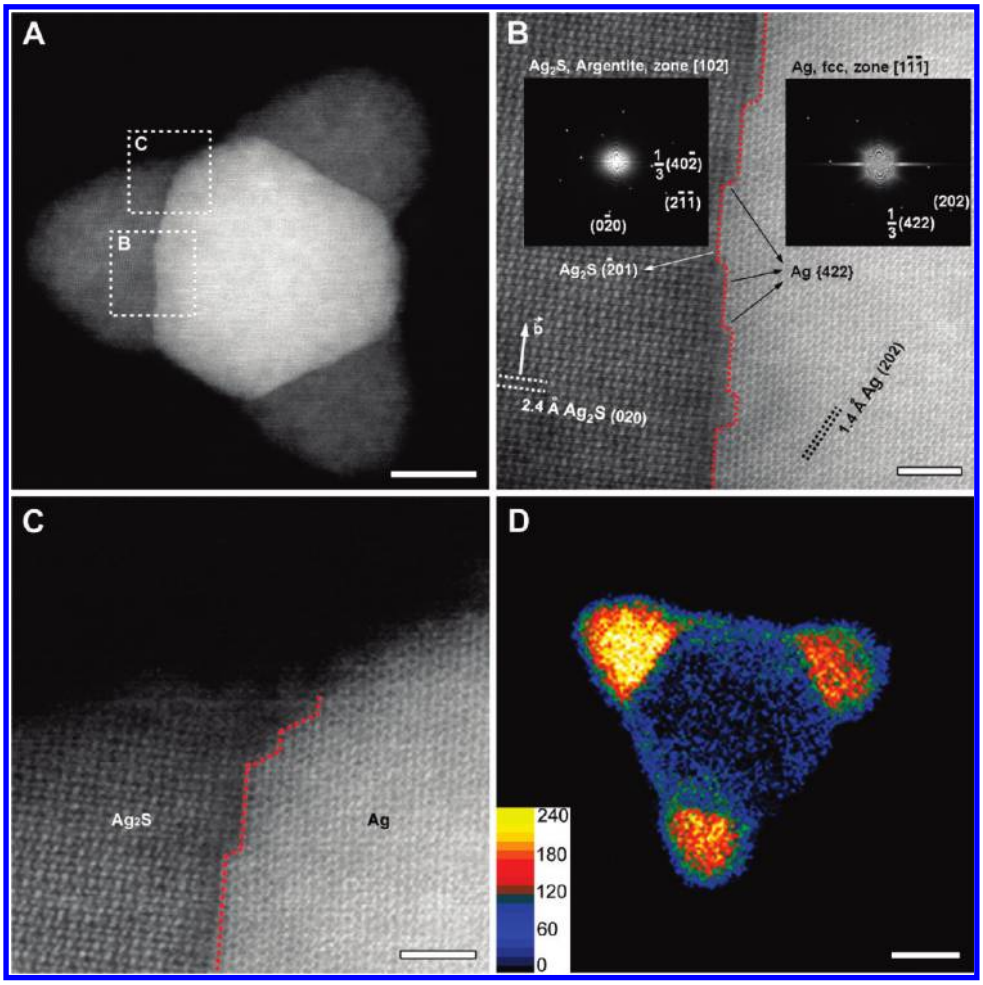

Figure 2. Electron microscopy characterization of the Ag–Ag_2S hybrid nanoplate obtained by stopping the sulfuration reaction at t = 1 min. (A) High-angle annular dark-field STEM image of a typical Ag–Ag_2S nanoplate, clearly showing selective sulfuration at all corner sites of the Ag nanoplate. (B,C) High-resolution STEM images of the Ag–Ag_2S nanoplate taken from the two regions marked in (A). The insets of (B) show Fourier transform patterns of the images along the [102] zone axis of Ag_2S and the [1$\bar{1}\bar{1}$] zone axis of Ag. The dotted red lines in (B,C) mark the boundary dividing the adjacent Ag and Ag_2S regions. (D) Color-composite energy-filtered TEM image of another Ag–Ag_2S nanoplate in the same sample, where the orange color corresponds to the highest concentration for S. The inset gives the color scale indicating the electron counts of the image. The scale bars are 10 nm in (A,D), and 2 nm in (B,C).

In a typical synthesis, we mixed an aqueous suspension of triangular Ag nanoplates with a specific amount of aqueous polysulfide, Na_2S_x, which was prepared in advance by reacting sulfur powders with an aqueous Na_2S solution at 80 °C for 12 h under ambient

dx.doi.org/10.1021/nl2016448 |*Nano Lett.* 2011, 11, 3010–3015

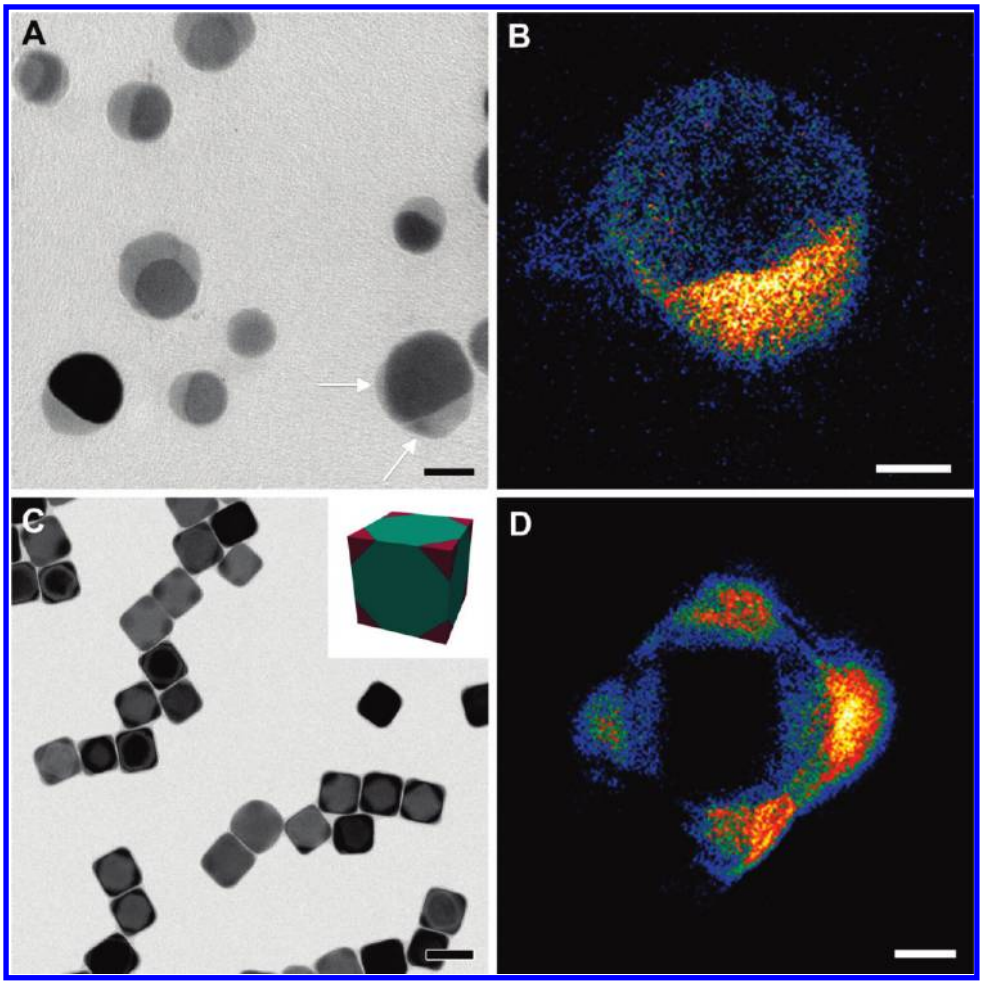

Figure 3. Sulfuration of Ag circular disks lacking sharp corners and Ag nanocubes with sharp corners. (A) TEM image of the product after sulfuration of the disks for 10 min, indicating that the reaction preferred to occur at one particular site of the disk. (B) Energy-filtered TEM image of a typical Ag−Ag_2S disk. (C) TEM image of the product after sulfuration of the Ag nanocubes for 20 min, showing that the reaction preferentially occurred at all corners of the nanocube. The inset shows an illustration of the Ag nanocube with Ag_2S formed at all corners. (D) Energy-filtered TEM image of a typical Ag−Ag_2S hybrid nanocube. The orange color in (B,D) corresponds to S with the same intensity scale as in Figure 2D. The scale bars are 20 nm in (A), 10 nm in (B, D), and 50 nm in (C).

conditions.[26] The reaction can be described by the following equation

$$2(x-1)\mathrm{Ag} + \mathrm{S}_x^{2-} \rightarrow (x-1)\mathrm{Ag_2S} + \mathrm{S}^{2-} \qquad (1)$$

On the basis of the change in Gibbs free energy ($\Delta G^\circ = -74.6$ kJ/mol at 298 K),[27,28] Ag_2S is expected to form spontaneously when elemental Ag and S_x^{2-} ions encounter and react in the absence of oxygen. Figure 1A shows a schematic of the sulfuration process and all major intermediate products we have observed. Figure 1B−E, shows transmission electron microscopy (TEM) images of the original, triangular nanoplates of Ag and a series of intermediate products collected by quenching the reaction at different time points. Evidently, sulfuration reaction was selectively initiated at the corner sites of a triangular nanoplate, followed by progression toward the central region. As the reaction time was expanded, the Ag_2S regions at corners increased continuously in area while the Ag region in the center shrank concurrently. With the ratio of Ag_2S to Ag increasing, the in-plane dipole plasmon peak of the Ag nanoplates experienced a continuous depression and a red shift while the short-wavelength absorption derived from the Ag_2S region became more prominent (Supporting Information Figure S1A) probably due to the high dielectric constant of Ag_2S.[29,30] In addition, the Ag−Ag_2S hybrid nanoplates exhibited a modified spatial pattern for the plasmonic modes in comparison with nanoplates made of pure Ag (for details, see Supporting Information and Figure S1B).

To reveal the sulfuration mechanism, we used a number of state-of-the-art imaging tools to characterize the structures and analyze the chemical compositions of the products obtained at different stages of a reaction. Figure 2A shows a high-angle annular dark-field (HAADF) scanning transmission electron microscopy (STEM) image of the product obtained at $t = 1$ min, where the bright and dark regions correspond to Ag and Ag_2S, respectively. Examination of the same sample by high-resolution STEM (Figure 2B,C) indicates that the sulfuration reaction resulted in a steplike interface between the neighboring Ag and Ag_2S regions. As marked by the dotted red lines, a majority of the interface was oriented parallel to the {422} planes of the face-centered cubic (fcc) lattice of Ag. The reciprocal lattices (the insets of Figure 2B) obtained from two-dimensional Fourier transform of the lattice-resolved images are in agreement with the $[1\bar{1}1]$ and [102] zone axes of fcc Ag and argentite Ag_2S,

dx.doi.org/10.1021/nl2016448 |*Nano Lett.* 2011, 11, 3010–3015

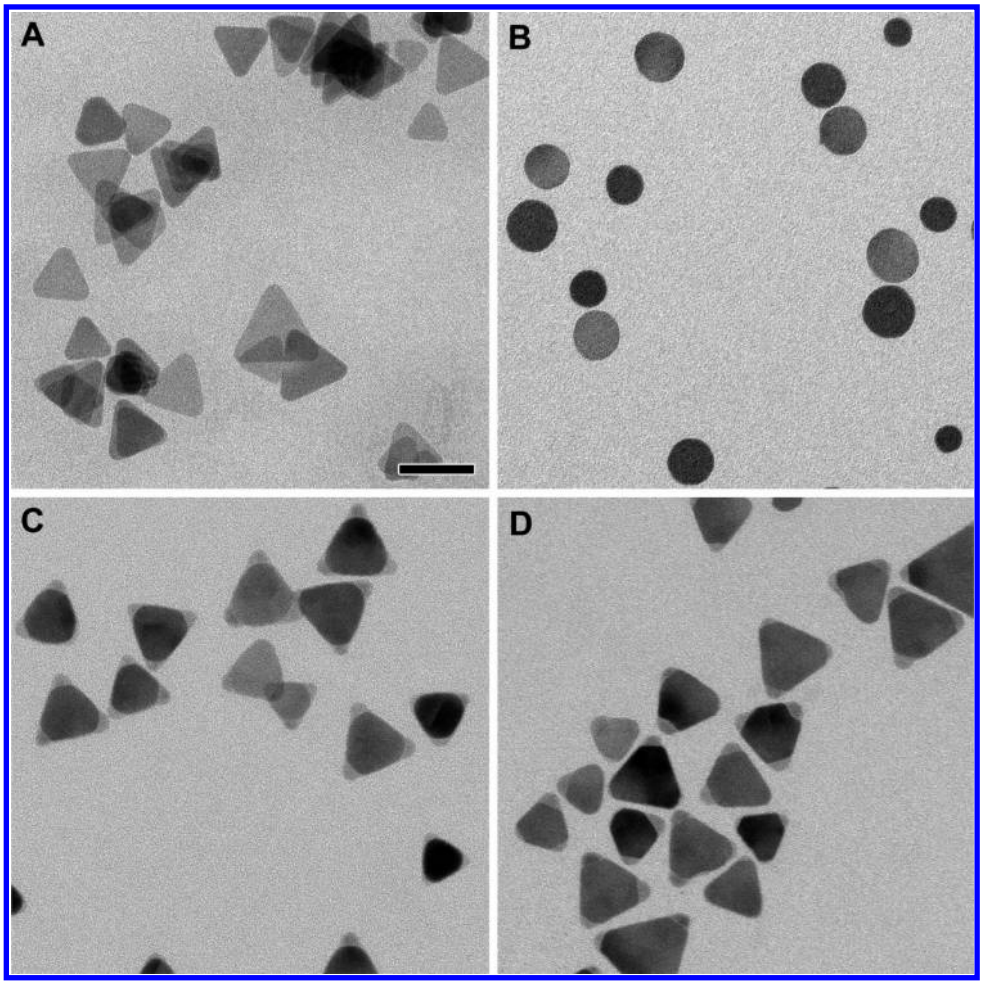

Figure 4. Comparison of the thermal stability of the triangular Ag and Ag−Ag_2S nanoplates. (A,B) TEM images of the triangular Ag nanoplates before and after they had been aged at 80 °C for 9 h. The sharp corners of the Ag nanoplates were rounded to generate circular disks with reduced lateral dimensions. (C,D) TEM images of the triangular Ag−Ag_2S nanoplates before and after they had been aged at 80 °C for 9 h. No distinct morphology change was observed before and after aging. The scale bar in (A) is 50 nm and applies to all images.

respectively. It is worth noting that the well-known stacking faults along the zone axis of a Ag nanoplate were also passed on to the Ag_2S regions. Specifically, the sets of spots with a spacing of 2.5 and 3.3 Å could be assigned to the 1/3{422} forbidden reflection of Ag and 1/3{40$\bar{2}$} forbidden reflection of Ag_2S, respectively.[31] The assignments of different regions to Ag and Ag_2S are also consistent with the energy-filtered mapping for S (Figure 2D), where the intensity of color is directly proportional to the amount of S^{2-}.

It is worth pointing out that the triangular shape was essentially preserved even though the lattice of Ag atoms underwent massive transformation during sulfuration. As a result, the S_x^{2-} species had to diffuse into the lattice of Ag atoms, most likely from both top and bottom surfaces of a nanoplate in order to continue the reaction. Thus, the reaction kinetics should be mainly determined by the diffusion rate of S_x^{2-} into the crystal lattices of Ag. Typically, S_x^{2-} has a much larger size (depends on the degree of polymerization) relative to the monomeric S or S^{2-} species,[32] and ultimately, S_x^{2-} can only diffuse into the Ag lattice very slowly, leading to a great reduction for the reaction rate and thus a well-controlled sulfuration rate. This kinetic difference represents one of the major advantages for our method relative to previous studies involving Na_2S.[24,25] Our observations are also in good agreement with the previous studies of polysulfide, where it was found both experimentally and theoretically that any increase in degree of polymerization or size could lead to a significant reduction in diffusion coefficient for the polysulfide species across an interface between sulfur and sodium polysulfide.[33,34]

Another obvious result is that the lateral dimensions of the Ag−Ag_2S nanoplates were larger than those of the original Ag nanoplates. On the basis of the molar volumes of Ag_2S and Ag (34.3 cm^3 /mol for Ag_2S and 10.3 cm^3 /mol Ag),[35] we anticipate that the volume of the Ag_2S region must be 70% larger than that of the original Ag region. Since the thickness of the Ag_2S region was essentially the same as the Ag region (Supporting Information Figure S2), there was only one possibility for the Ag_2S region to expand its volume during the sulfuration reaction, that is, increasing its area laterally. This argument is supported by the observations in Figure 1C−E and Figure 2A. Once the Ag_2S regions had started to appear at the corners of a triangular Ag nanoplate, they could grow in area until they met in the center of the plate as long as sufficient sulfur was supplied. The simultaneous reactions at different sites of a nanoplate indubitably increased the internal energy due to the strain at the interface caused by the lattice mismatch between Ag and Ag_2S. However, it is likely that the shape of the nanoplate plays a more important

dx.doi.org/10.1021/nl2016448 |*Nano Lett.* 2011, 11, 3010–3015

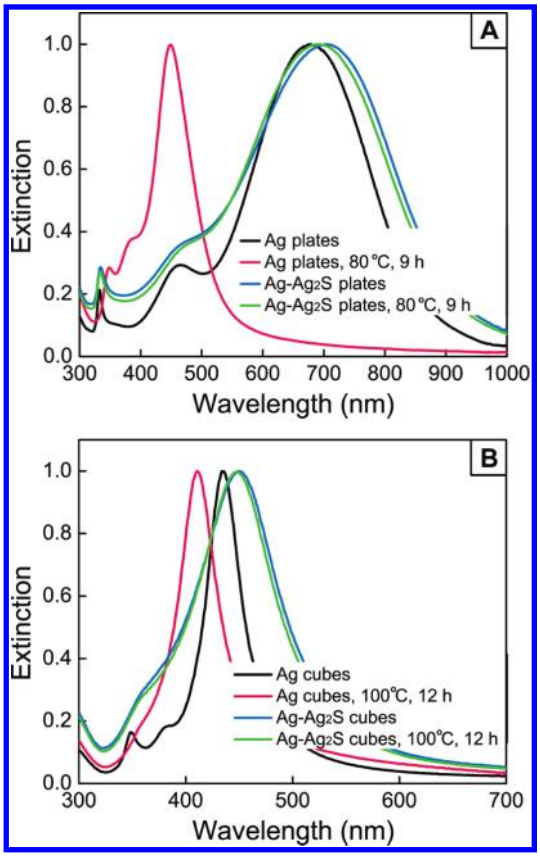

Figure 5. (A) Extinction spectra recorded from aqueous suspensions of the Ag nanoplates and Ag−Ag_2S nanoplates before and after the samples had been aged at 80 °C for 9 h. The samples correspond to those shown in Figure 4A−D. (B) Extinction spectra recorded from aqueous suspensions of the Ag nanocubes and Ag−Ag_2S nanocubes before and after the samples had been aged at 100 °C for 12 h. The samples of Ag nanocubes and Ag−Ag_2S nanocubes correspond to those shown in Supporting Information Figure S4 and Figure 3C.

role than the strain in determining the sites of initiation for sulfuration.

To understand the effect of sharp corners on the site selectivity of sulfuration, we also investigated the reactions between S_x^{2-} and Ag nanoplates with a rounded profile (Supporting Information Figure S3). In the case of a triangular Ag nanoplate, the sharp corners with a small curvature radius can serve as the nucleation sites for reaction with S_x^{2-} due to the relatively high energy and thus activity at these sites. However, it is a different situation for a circular disk of Ag that lacks sharp corners on the surface. In this case, S_x^{2-} tends to react with the elemental Ag randomly on the surface (or edge) of a disk, the subsequent diffusion of S_x^{2-} and its reaction with Ag would preferentially continue at this specific site rather than to start the reaction at a new site. This preference can be attributed to the increase in internal energy induced by the interfacial strain between Ag and Ag_2S. As a result, the reaction would predominately occur at a single site on a circular disk (see Figure 3A,B). In fact, we could only find very few Ag disks containing two Ag_2S regions on the same plate, as indicated by white arrows in Figure 3A. Comparing the results from both triangular nanoplates and circular disks of Ag, we can conclude that the reaction tends to be initiated from a corner site with a small curvature radius. It is also worth noting that the sulfuration of circular Ag disks (it took ~10 min to generate the hybrid structure shown in Figure 3A) was much slower than that of triangular Ag nanoplates (which only took 1 min to obtain the structure shown in Figure 1C). This large difference in sulfuration rate also indicates a relatively higher activity at the corner sites. The same trend was also observed in the sulfuration of Ag nanospheres and nanocubes.

In addition to the two-dimensional system like thin nanoplates, we have also successfully extended the new sulfuration method to a three-dimensional system by generating Ag−Ag_2S hybrid nanocubes. As expected, the TEM image in Figure 3C and the S elemental mapping in Figure 3D indicate that the sulfuration reaction was also initiated from all the corner sites of a Ag nanocube and the reaction kinetics and the degree of sulfuration could be easily controlled. It is worth pointing out that, the Ag−Ag_2S hybrid nanocubes could also tolerate large mismatch in lattice constants without forming dislocations or losing the original shape.

Interestingly, both triangular nanoplates and nanocubes of Ag exhibited enhanced thermal stability against aging after their corner sites had been selectively converted into Ag_2S via sulfuration with Na_2S_x. As shown in Figure 4A,B, the original triangular Ag nanoplates suffered a significant change to their morphology by rounding their sharp corners when they were dispersed in water and aged at 80 °C for 9 h.[8] However, the Ag−Ag_2S hybrid nanoplates were able to retain their triangular shape under the same aging conditions (Figure 4C,D). These changes were also reflected in their LSPR spectra recorded with a UV−vis spectrometer. The in-plane dipole peak was blue shifted more than 300 nm in the case of triangular Ag nanoplates, while the peak was changed very little for the Ag−Ag_2S hybrid nanoplates (Figure 5A). Again, the same trend was also observed for Ag nanocubes without and with sulfuration at the corner sites (Figure 5B).

In conclusion, we have demonstrated an effective approach to site-selected modification of Ag nanocrystals by sulfuration with S_x^{2-} at the corner sites. In comparison with previous studies involving S^{2-} and oxygen, both the kinetics and degree of sulfuration could be better controlled by switching to S_x^{2-}. With triangular nanoplates and nanocubes of Ag as two examples, we clearly showed that sharp corners played an important role in determining the initiation sites for sulfuration. Our studies also revealed that the Ag_2S formed at the corners of Ag nanocrystals could effectively prevent the nanocrystals from changing their shapes during an aging process and thus improve their thermal stability, a feature vital to various applications in plasmonics and catalysis. Considering the high affinity of noble metals to sulfur,[36,37] the concept demonstrated here is potentially extendable to many other systems.

■ ASSOCIATED CONTENT

Supporting Information. Additional information and figures. This material is available free of charge via the Internet at http://pubs.acs.org.

■ AUTHOR INFORMATION

Corresponding Author
*E-mail: xia@biomed.wustl.edu.

■ ACKNOWLEDGMENT

This work was supported in part by a research grant from the NSF (DMR-0804088) and startup funds from Washington

University in St. Louis. Part of the research was performed at the Nano Research Facility (NRF), a member of the National Nanotechnology Infrastructure Network (NNIN), which is supported by the National Science Foundation under NSF Award No. ECS-0335765. Y.X. was also partially supported by the World Class University (WCU) program through the National Research Foundation of Korea funded by the Ministry of Education, Science and Technology (R32-20031). The work at BNL was supported by the U.S. Department of Energy (Basic Energy Sciences) and by the Materials Science and Engineering Division under Contract No. DE-AC02-98CH10886 and through the use of CFN.

REFERENCES

(1) He, J.; Ichinose, I.; Kunitake, T.; Nakao, A.; Shiraishi, Y.; Toshima, N. *J. Am. Chem. Soc.* **2003**, *125*, 11034.
(2) Christopher, P.; Linic, S. *J. Am. Chem. Soc.* **2008**, *130*, 11264.
(3) Lei, Y.; Mehmood, F.; Lee, S.; Greeley, J.; Lee, B.; Seifert, S.; Winans, R. E.; Elam, J. W.; Meyer, R. J.; Redfern, P. C.; Teschner, D.; Schlogl, R.; Pellin, M. J.; Curtiss, L. A.; Vajda, S. *Science* **2010**, *328*, 224.
(4) Christopher, P.; Xin, H.; Linic, S. *Nat. Chem.* **2011**, *3*, 467.
(5) Wu, Y.; Li, Y.; Ong, B. S. *J. Am. Chem. Soc.* **2007**, *129*, 1862.
(6) Tao, A. R.; Sinsermsuksakul, P.; Yang, P. *Nat. Nanotechnol.* **2007**, *2*, 435.
(7) Peng, H.-I.; Strohsahl, C. M.; Leach, K. E.; Krauss, T. D.; Miller, B. L. *ACS Nano* **2009**, *3*, 2265.
(8) Zeng, J.; Robert, S.; Xia, Y. *Chem.—Eur. J.* **2010**, *16*, 12559.
(9) Sun, Y.; Xia, Y. *Science* **2002**, *298*, 2176.
(10) Jin, R.; Cao, Y.; Mirkin, C. A.; Kelly, K. L.; Schatz, G. C.; Zheng, J. G. *Science* **2001**, *294*, 1901.
(11) Jin, R.; Cao, Y. C.; Hao, E.; Métraux, G. S.; Schatz, G. C.; Mirkin, C. A. *Nature* **2003**, *425*, 487.
(12) Hu, J.-Q.; Chen, Q.; Xie, Z.-X.; Han, G.-B.; Wang, R.-H.; Ren, B.; Zhang, Y.; Yang, Z.-L.; Tian, Z.-Q. *Adv. Funct. Mater.* **2004**, *14*, 183.
(13) Wiley, B.; Sun, Y.; Xia, Y. *Acc. Chem. Res.* **2007**, *40*, 1067.
(14) Pietrobon, B.; Kitaev, V. *Chem. Mater.* **2008**, *20*, 5186.
(15) Zeng, J.; Zheng, Y.; Rycenga, M.; Tao, J.; Li, Z.-Y.; Zhang, Q.; Zhu, Y.; Xia, Y. *J. Am. Chem. Soc.* **2010**, *132*, 8552.
(16) Tao, A.; Sinsermsuksakul, P.; Yang, P. *Angew. Chem., Int. Ed.* **2006**, *45*, 4597.
(17) Gao, Y.; Jiang, P.; Song, L.; Wang, J. X.; Liu, L. F.; Liu, D. F.; Xiang, Y. J.; Zhang, Z. X.; Zhao, X. W.; Dou, X. Y.; Luo, S. D.; Zhou, W. Y.; Xie, S. S. *J. Cryst. Growth* **2006**, *289*, 376.
(18) Cobley, C.; Rycenga, M.; Zhou, F.; Li, Z.-Y.; Xia, Y. *Angew. Chem., Int. Ed.* **2009**, *48*, 4824.
(19) Zeng, J.; Xia, X.; Rycenga, M.; Henneghan, P.; Li, Q.; Xia, Y. *Angew. Chem., Int. Ed.* **2011**, *50*, 244.
(20) Chen, J.; McLellan, J. M.; Siekkinen, A.; Xiong, Y.; Li, Z.-Y.; Xia, Y. *J. Am. Chem. Soc.* **2006**, *128*, 14776.
(21) Xiong, Y. *Chem. Commun.* **2011**, *47*, 1580.
(22) Zhang, Q.; Ge, J.; Pham, T.; Goebl, J.; Hu, Y.; Lu, Z.; Yin, Y. *Angew. Chem., Int. Ed.* **2009**, *48*, 3516.
(23) Christopher, P.; Linic, S. *ChemCatChem* **2010**, *2*, 78.
(24) Seo, D.; Choong, I. Y.; Jung, J.; Song, H. *J. Am. Chem. Soc.* **2008**, *130*, 2940.
(25) Liu, B.; Ma, Z. *Small* **2011**10.1002/smll.201100095.
(26) Oei, D. G. *Inorg. Chem.* **1973**, *12*, 438.
(27) Kubaschewski, O.; Alcock, C. B.; Spenser, P. J. *Materials Thermochemistry*; Pergamon Press: New York, 1993.
(28) Wagman, D. D.; Evans, W. H.; Parker, V. B.; Schumm, R. H.; Halow, I.; Bailey, S. M.; Churney, K. L.; Nuttall, R. L. The NBS Tables of Chemical Thermodynamic Properties. *J. Phys. Chem. Ref. Data* **1982**, *11*, Suppl. 2.
(29) Pastoriza-Santos, I.; Liz-Marzán, L. M. *Nano Lett.* **2002**, *2*, 903.
(30) Burda, C.; Chen, X.; Narayanan, R.; El-Sayed, M. A. *Chem. Rev.* **2005**, *105*, 1025.
(31) Wang, Z. L. *J. Phys. Chem. B* **2000**, *104*, 1153.
(32) Takeda, N.; Tokitoh, N.; Okazaki, R. *Top. Curr. Chem.* **2003**, *231*, 153.
(33) Divisek, J.; Bodewig, F. G.; Mergel, J.; Lippert, H.; Kastening, B. *J. Electrochem. Soc.* **1980**, *127*, 357.
(34) Thompson, S.; Newman, J. *J. Electrochem. Soc.* **1989**, *136*, 3362.
(35) Weast, R. C. *The CRC Handbook of Chemistry and Physics*; CRC Press: Cleveland, OH, 1974.
(36) Yin, Y.; Rioux, R. M.; Erdonmez, C. K.; Hughes, S. M.; Somorjai, G. A.; Alivisatos, A. P. *Science* **2004**, *304*, 711.
(37) Son, D.; Hughes, S. M.; Yin, Y.; Alivisatos, A. P. *Science* **2004**, *306*, 1009.